Energetics and Mechanisms of Carbon–Carbon and Carbon–Iodide Reductive Elimination from a Pt(IV) Center

Karen I. Goldberg,*,† JiYang Yan, and Eric M. Breitung

Contribution from the Department of Chemistry, Illinois State University, Normal, Illinois 61790-4160

Received August 12, 1994. Revised Manuscript Received December 29, 1994[⊗]

Abstract: Thermolysis of dppePtMe$_3$I (**1**, dppe = $Ph_2PCH_2CH_2PPh_2$) in both solid state and solution (acetone-d_6) results in competitive methyl iodide and ethane production. The expected Pt(II) products of these reductive elimination reactions, dppePtMe$_2$ (**2**) and dppePtMeI (**3**), are also observed. In the presence of added iodide (in acetone-d_6), the carbon–carbon bond forming reductive elimination reaction is substantially inhibited, and an equilibrium is established between **1** and the carbon–iodide reductive elimination products, **2**/MeI. Thermodynamic and kinetic parameters for the reductive elimination of methyl iodide from **1** were measured under these conditions ($\Delta H = 66 \pm 3$ kJ/mol, $\Delta S = 153 \pm 7$ J/(mol·K); $\Delta H_{re}^{\ddagger} = 104 \pm 1$ kJ/mol, $\Delta S_{re}^{\ddagger} = -12 \pm 1$ J/(mol·K)). Estimates of the enthalpy of the carbon–carbon reductive elimination reaction ($\Delta H = -105$ kJ/mol) and of Pt^{IV}–C and Pt^{IV}–I bond strengths (132 and 196 kJ/mol, respectively) were made from DSC data. Mechanistic studies of the solution thermolysis support the involvement of a common five-coordinate cationic intermediate (formed by dissociation of iodide), from which both carbon–carbon and carbon–iodide elimination products result. Exclusive production of methyl iodide or ethane can be achieved by the addition or removal of iodide, respectively, from the reaction.

Introduction

Although a considerable amount of information is available on oxidative addition reactions involving unsaturated metal centers, the microscopic reverse—reductive elimination—has received much less attention and investigation.[1] This situation is especially true for the oxidative addition/reductive elimination reactions of alkyl halides, and it is likely a result of thermodynamic factors. Oxidative addition of alkyl halides is generally enthalpically favored, and thus study of the reductive elimination reaction is often not feasible. However, the elimination and coupling of alkyl– or acyl–halide groups from transition metals is of great importance in catalysis and transition metal mediated organic synthesis. For example, the coupling of an alkyl group with a chloride from a Rh(III) intermediate is suggested as the product-forming step in the decarbonylation of certain acid chlorides.[1] The mechanism proposed for the Monsanto Acetic Acid Synthesis (often cited as one of the most industrially significant applications of homogeneous transition metal catalysis) involves oxidative addition of methyl iodide in the first step and reductive elimination of acetyl iodide in the final metal mediated step.[1,2] Thus extending our understanding of the energetics and mechanisms of reductive elimination reactions in general, and of C–X reductive elimination in particular, would be of considerable benefit.

Scheme 1

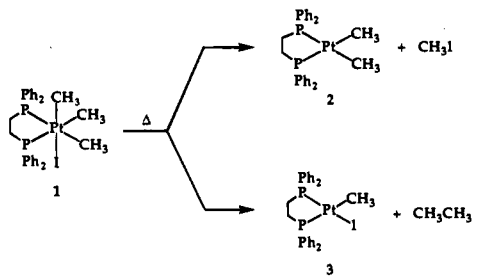

Recently we reported that thermolysis of dppePtMe$_3$I (**1**, dppe = $Ph_2PCH_2CH_2PPh_2$) resulted in competitive carbon–iodide and carbon–carbon reductive elimination reactions producing methyl iodide/dppePtMe$_2$ (**2**) and ethane/dppePtMeI (**3**), respectively (Scheme 1).[3] It was observed that in the presence of excess iodide in acetone solution, an equilibrium between **1** and **2**/MeI is established. This has allowed us to study the microscopic reverse of one of the most thoroughly investigated oxidative addition reactions, oxidative addition of methyl iodide to square-planar d^8 metal centers. In addition, due to the competitive nature of the alkyl–alkyl and alkyl–halide elimination reactions from the same metal complex, we were able to directly compare the thermodynamics, kinetics, and mechanisms of carbon–carbon and carbon–halide reductive elimination reactions. Given that species in catalytic cycles often contain multiple alkyl and halide groups, further understanding of the energetics and mechanisms of these potentially competing elimination reactions is desirable for the rational design of future catalysts. In this contribution we describe the measurement of thermodynamic and kinetic parameters for the eliminations and present strong evidence that the mechanisms of both eliminations involve a five-coordinate cationic intermediate formed by dissociation of iodide. The addition or removal of iodide from the system can thus be used to "control" the competition and yield only one set of elimination products.

† Current address: Department of Chemistry, Box 357100, University of Washington, Seattle, WA 98195-1700.

⊗ Abstract published in *Advance ACS Abstracts*, June 15, 1995.

(1) For reviews and chapters on oxidative addition/reductive elimination reactions see: (a) Collman, J. P.; Hegedus, L. S.; Norton, J. R.; Finke, R. G. *Principles and Applications of Organotransition Metal Chemistry*; University Science Books: Mill Valley, CA, 1987. (b) Lukehart, C. M. *Fundamental Transition Metal Organometallic Chemistry*; Brooks/Cole: Monterey, CA, 1985. (c) Stille, J. K. In *The Chemistry of the Metal–Carbon Bond*; Hartley, F. R., Patai, S., Eds.; Wiley: New York, 1985; Vol. 2. (d) Atwood, J. D. *Inorganic and Organometallic Reaction Mechanisms*; Brooks/Cole: Monterey, CA, 1985. (e) Crabtree, R. H. *The Organometallic Chemistry of the Transition Metals*; Wiley: New York, 1988.

(2) (a) Forster, D. *Adv. Organomet. Chem.* **1979**, *17*, 255. (b) Haynes, A; Mann, B. E.; Morris, G. E.; Maitlis, P. M. *J. Am. Chem. Soc.* **1993**, *115*, 4093 and references therein.

(3) Goldberg, K. I.; Yan, J. Y.; Winter, E. L. *J. Am. Chem. Soc.* **1994**, *116*, 1573.

0002-7863/95/1517-6889$09.00/0

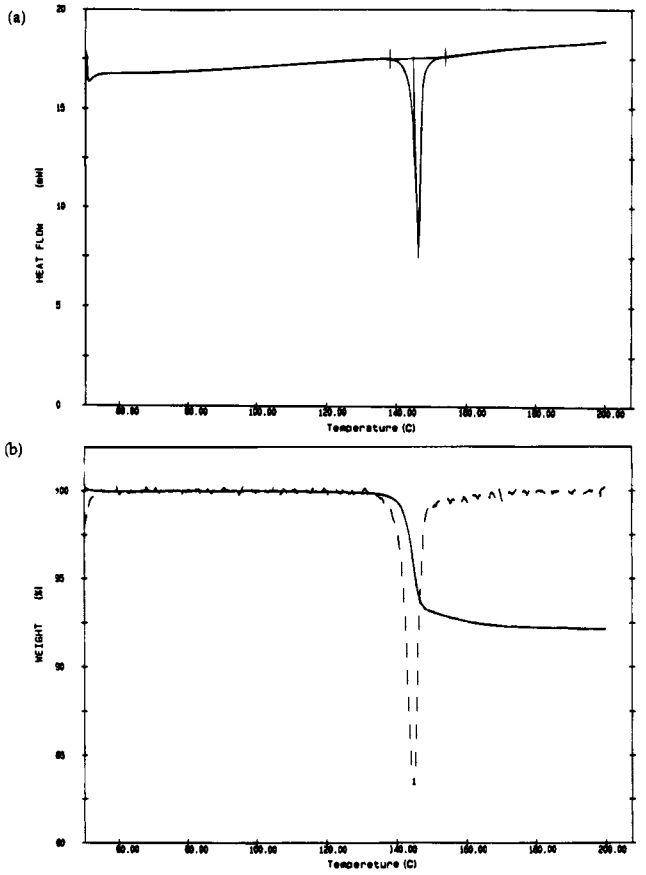

Figure 1. Solid state thermal decomposition of dppePtMe$_3$I (**1**): (a) differential scanning calorimetry (DSC); (b) thermogravimetric analysis (TGA) (dashed line is first derivative of data).

Results and Discussion

Solid State Pyrolysis of dppePtMe$_3$I. Pyrolysis of solid samples of **1** was monitored by differential scanning calorimetry (DSC) and thermogravimetric analysis (TGA). A single exotherm at 146 °C was observed in the range 50−200 °C (Figure 1a) and the enthalpy of the decomposition reaction was found to be $\Delta H_{obs} = -69.2 \pm 0.6$ kJ/mol. The solid residues that remained after the DSC experiments were examined by ^{1}H NMR ($CDCl_3$) and signals for two Pt(II) products were observed: dppePtMe$_2$ (**2**) and dppePtMeI (**3**). The mole ratio of these Pt(II) products (determined by integration of the Pt-CH_3 signals) was 18/82 dppePtMe$_2$ (**2**)/dppePtMeI (**3**). As **2** is the Pt product expected for carbon−iodide coupling reductive elimination and **3** is the Pt product expected for carbon−carbon coupling reductive elimination, interpretation of this datum is that ethane is lost preferentially to methyl iodide by an 82/18 ratio under solid state pyrolysis conditions.

The numerical value of this ratio was confirmed in TGA experiments. In the temperature range 50−200 °C, only one weight loss transition was observed (at 145 °C) with a 6.8 ± 0.2% weight loss (Figure 1b). The solid residues from these trials were also examined by ^{1}H NMR ($CDCl_3$) and the same product ratio of 82/18 for dppePtMeI/dppePtMe$_2$ was confirmed. Additional verification that these are the *only* two products *and* that elimination proceeds with this ratio of products is obtained by calculation of the theoretical weight loss expected upon 82% production of ethane and 18% production of methyl iodide. The calculated value of 6.6% is within experimental error of the observed value. A weight loss of only 3.9% would be expected if 100% loss of ethane had occurred.

The resulting solid residues consisting of **2** and **3** were also monitored by DSC and TGA in the temperature range 50−200 °C. No phase changes or decomposition was observed for these species below 200 °C.[4] Thus the ΔH measured for the pyrolysis of dppePtMe$_3$I corresponds to the weighted sum of the enthalpies of the two reductive elimination processes (eq 1)

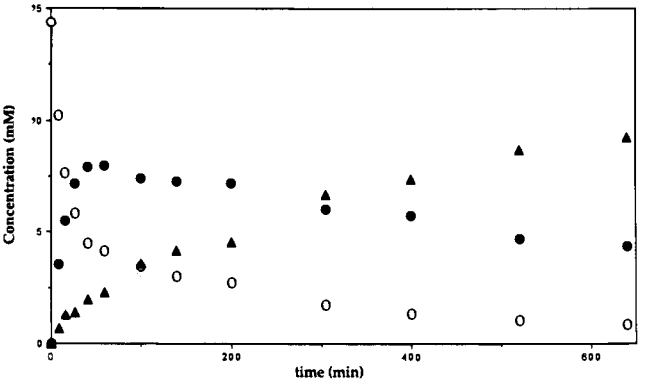

Figure 2. Solution thermolysis of **1** in acetone-d_6 at 79 °C. Concentrations of reactant and products as a function of time: [dppePtMe$_3$I (**1**, open circles), dppePtMe$_2$ (**2**, filled circles), and dppePtMeI (**3**, triangles)].

$$\Delta H_{obs} = -69.2 \text{ kJ/mol} = (0.82)\Delta H_{C-C} + (0.18)\Delta H_{C-I} \quad (1)$$

In reference to eq 1, ΔH_{C-C} is the enthalpy of the carbon−carbon coupling reaction producing ethane/dppePtMeI, and ΔH_{C-I} is the enthalpy of the carbon−iodide coupling reaction producing methyl iodide/dppePtMe$_2$.

Our solid state results differ significantly from those reported by Puddephatt et al. for the pyrolysis of **1**, where ethane was evolved at 215−220 °C and quantified at 96%.[5] The solid residue remaining was identified as pure dppePtMeI (**3**) by its melting point (243−245 °C) and NMR spectrum. However, the ^{1}H NMR spectral data reported for **3** by these authors are actually that for dppePtMe$_2$ (**2**) [($CDCl_3$) δ 0.69 (t, $J_{P-H} = 7.2$ Hz, $J_{Pt-H} = 72$ Hz), see Experimental Section]. Assuming that this entry in the table was an oversight and that the residue was exclusively dppePtMeI, a possible explanation for the difference in our results might simply be a difference in heating methods. Both the DSC and the TGA operate with a nitrogen flow which would carry away any methyl iodide that was produced. If their sample was heated in a closed system, any methyl iodide produced could react with dppePtMe$_2$ and regenerate starting material which could further react to irreversibly eliminate ethane.

Solution State Thermolysis of dppePtMe$_3$I. The solution thermolysis of **1** in acetone-d_6 (sealed system) was monitored by ^{1}H NMR. Similar to the solid state experiments, products resulting from both carbon−carbon and carbon−iodide bond forming reductive elimination were observed. The product ratios, however, varied with time and the concentrations of the starting material **1** and the two Pt(II) products **2** and **3** are shown as a function of reaction time in Figure 2. Although the concentration of starting material, **1**, decreased steadily with reaction time, and the concentration of the Pt(II) product resulting from carbon−carbon coupling, dppePtMeI (**3**), increased steadily with reaction time, the concentration of the Pt(II) product resulting from carbon−iodide coupling, dppePtMe$_2$ (**2**), increased to a maximum at early reaction times and then decreased as the reaction continued. In addition, while the

(4) This is consistent with the reported melting points of **2** (215−216 °C,[4a] 221−223 °C[4b]) and **3** (243−245 °C[4a,c]). (a) Hooten, K. A., *J. Chem. Soc. A* **1970**, 1896. (b) Clark, H. C.; Jablonski, C. R. *Inorg. Chem.* **1975**, *14*, 1518. (c) Reference 5

(5) Brown, M. P.; Puddephatt, R. J.; Upton, C. E. E. *J. Chem. Soc., Dalton Trans.* **1974**, 2457.

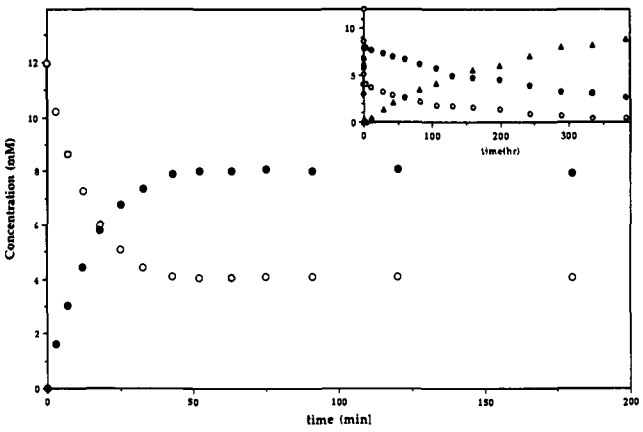

Figure 3. Solution thermolysis of **1** in acetone-d_6 at 79 °C with [NaI] = 0.30 M. Concentrations of reactant and products as a function of time: [dppePtMe$_3$I (**1**, open circles), dppePtMe$_2$ (**2**, filled circles), and dppePtMeI (**3**, triangles)]. Inset plot shows longer reaction times (hours).

concentration of **2** is greater than that of **3** at early reaction times (at less than 30% conversion of **1**, MeI and **2** comprised from 60 to 80% of the elimination products), eventually all material is converted to the carbon−carbon coupling products, **3** and ethane.

When iodide was added to the reaction system, the carbon-carbon coupling pathway was substantially inhibited. As shown in Figure 3, during the early part of the reaction only the carbon−iodide products (dppe)PtMe$_2$ (**2**) and MeI were observed. The reaction reached an equilibrium between **1** and **2** + MeI which was maintained for several hours before any of the carbon−carbon coupling products, **3** and ethane, were observed. In comparing Figures 2 and 3 it can be seen that the time at which the carbon−iodide coupling products, (dppe)-PtMe$_2$ (**2**) and MeI, reached their maximum concentration in the reaction without added iodide (45 min at 79 °C) is nearly identical to the time that equilibrium concentrations were established in the presence of iodide (43 min at 79 °C). In addition, the time at which equilibrium was reached proved to be virtually independent of the iodide concentration. For example, as [NaI] was varied from 0.17 to 0.30 M at 79 °C, equilibrium was consistently reached at 43 min, and at 89 °C, with [NaI] from 0.060 to 0.27 M, equilibrium was reached at 28 min. Thus, although iodide ions were seen to strongly inhibit the carbon−carbon coupling reductive elimination pathway, their presence had little effect on the carbon−iodide coupling reductive elimination pathway. Eventually, however, even in the presence of excess iodide, all material converted to the carbon−carbon reductive elimination products (Figure 3, inset).

Equilibrium Constants and Thermodynamic Parameters of Methyl Iodide Elimination from 1. The concentrations of **1** and **2** were monitored via ^{1}H NMR spectrometry during the period that iodide rich thermolyses maintained equilibrium behavior. Equilibrium constants (K_{eq} = $[\mathbf{2}]_{eq}[MeI]_{eq}/[\mathbf{1}]_{eq}$ = $([\mathbf{2}]_{eq})^2/[\mathbf{1}]_{eq}$) were then calculated from the average values of these concentrations at temperatures between 69 and 99 °C (Table 1). As expected, there was no dependence of the equilibrium constants on the iodide concentration. However, equilibrium was maintained longer in the presence of higher iodide concentrations. For example at 89 °C, with [NaI] = 0.27 M, equilibrium concentrations were observed for at least 120 min, while with [NaI] = 0.060 M, equilibrium behavior was limited to *ca.* 70 min.

The enthalpy and entropy of the reaction were determined from the temperature dependence of the equilibrium constants. A van't Hoff plot is shown in Figure 4 and the enthalpy and

Table 1. Equilibrium and Rate Constants for the Reductive Elimination of Methyl Iodide from **1**

temp (°C)	initial [1] (10^3 M)	[NaI] (M)	K_{eq} (10^3 M)[a]	k_{re} (10^4 s^{-1})[a]
69.0	13	0.18−0.31	7.96 ± 0.04	2.36 ± 0.1
79.0	12−15	0.17−0.30	15.6 ± 0.4	6.82 ± 0.2
89.0	10−12	0.060−0.27	31.7 ± 0.3	19.1 ± 0.1
99.0	11−12	0.17−0.37	50.2 ± 0.4	48.2 ± 3

[a] Values are averages from 2 to 3 experiments (varying [NaI]) and error limits are one standard deviation from the average.

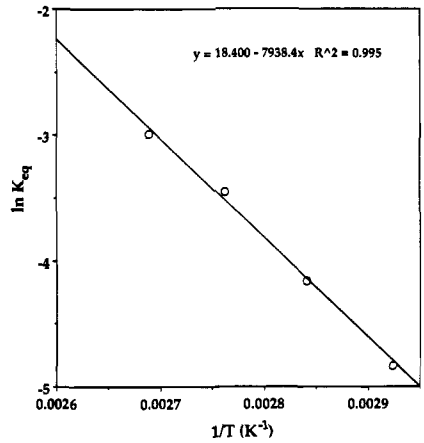

Figure 4. The dependence of ln(K_{eq}) on temperature for the reaction **1** ⇌ **2** + MeI.

entropy of methyl iodide elimination from **1** were calculated from these data: ΔH = 66 ± 2 kJ/mol and ΔS = 153 ± 7 J/(mol·K). The absolute magnitude of ΔH_{C-I} is approximately half of ΔH = −118 ± 8 kJ/mol measured for the oxidative addition of MeI to *trans*-IrCl(CO)(PMe$_3$)$_2$.[6] The relatively small enthalpy difference in the dppePtMe$_3$I ⇌ dppePtMe$_2$/MeI system allows observation of the reductive elimination reaction and the equilibrium behavior.

Estimates of the Enthalpy of Ethane Elimination from 1 and of Bond Energies. As the elimination of methyl iodide has been shown to be endothermic and the DSC results indicate a strong exotherm resulting from the combined methyl iodide and ethane elimination, the elimination of ethane must be strongly exothermic. Furthermore, we can estimate the magnitude of ΔH for the ethane elimination from the DSC data and the enthalpy of the solid state methyl iodide elimination. The value of the enthalpy of the methyl iodide elimination in the solid state (**1**(s) → **2**(s) + MeI(g)) can be approximated by its solution state value with a correction for the enthalpy of vaporization of methyl iodide[7] as shown below:

1(soln) → **2**(soln) + MeI(soln)	ΔH_1 = 66 ± 3 kJ/mol
1(s) → **1**(soln)	ΔH_2
2(soln) → **2**(s)	$\Delta H_3 \approx -\Delta H_2$
MeI(soln) → MeI(liq)	$\Delta H_4 \approx 0$
MeI(liq) → MeI(g)	ΔH_5 = 28.0 ± 1.3 kJ/mol[7]
1(s) → **2**(s) + MeI(g)	ΔH_{C-I}(solid state) ≈ 94 kJ/mol

In this approximation of ΔH_{C-I}(solid state), we are assuming that $\Delta H_{solution}$ of the Pt(IV) and the Pt(II) complexes are nearly equal ($\Delta H_2 \approx -\Delta H_3$) and that $\Delta H_{solution}$ of MeI in acetone is small enough to be neglected ($\Delta H_4 \approx 0$).[8] The value of ΔH_{C-I}(solid state) = 94 kJ/mol can then be substituted into eq 1 allowing the enthalpy of the carbon−carbon coupling reductive

(6) Yoneda, G.; Blake, D. M. *Inorg. Chem.* **1981**, *20*, 67
(7) Cox, J. D.; Picher, G. *Thermochemistry of Organic and Organometallic Compounds*; Academic Press: New York, 1970.

elimination reaction to be approximated at $\Delta H_{C-C} = -105$ kJ/mol. It is interesting that this value of ΔH is so close to the exothermic enthalpy $\Delta H = -113$kJ/mol predicted by generalized valence bond (GVB) theory for the elimination of ethane from the model Pt(IV) complex, $PtCl_2(CH_3)_2(PH_3)_2$.[9] That the carbon−carbon coupling products dppePtMeI/C_2H_6 are thermodynamically stable relative to the starting material dppePtMe$_3$I as well as to the carbon-iodide coupling products dppePtMe$_2$/MeI is consistent with our observations that in solution phase reactions where the methyl iodide and **2** remain in solution, eventually all material is converted to **3** and ethane.

Estimates of the Pt−CH_3 and the Pt−I bond energies can be made from the enthalpies of the reductive elimination reactions. For the carbon−carbon coupling reductive elimination leading to **3** and ethane, the enthalpy of the reaction can be approximated as arising from the cleavage of two Pt−CH_3 bonds and formation of the C−C bond in ethane: $\Delta H_{c-c} = 2\,D(\text{Pt-CH}_3) - D(\text{CH}_3 - \text{CH}_3)$. Substituting $D(CH_3-CH_3) = 368$ kJ/mol[10] and our value of −105 kJ/mol for ΔH_{c-c} provides an estimate of the Pt−CH_3 bond strength of 132 kJ/mol. This value is very close to $Pt^{IV}-CH_3$ bond strengths recently obtained by similar methods (137 and 125 kJ/mol) for the tetramethyl complexes, *cis*-$PtMe_4L_2$ (L = MeNC and 2,6-$Me_2C_6H_3NC$).[11] In addition, the value is almost identical to the $Pt^{IV}-CH_3$ bond strength (134 kJ/mol) predicted by GVB theory for the model complex, $PtCl_2(CH_3)_2(PH_3)_2$.[9] However, the $Pt^{IV}-C$ bond strength value that we found is lower than that reported for a monodentate phosphine analog of the iodotrimethyl complex **1**; the value of 153 kJ/mol was calculated for the Pt−CH_3 bond in (Me_2PhP)$_2$PtMe$_3$I.[12] Our value is also significantly lower than that determined for the $Pt^{IV}-CH_3$ bond in $CpPt(CH_3)_3$ (163 kJ/mol).[13] However, as previously discerned by Hoff *et al.*, after observing that $Ir^{III}-X$ bond strengths in Cp*(PMe_3)IrX_2 were approximately 80 kJ/mol greater than those in $(PR_3)_2CO(Cl)IrX_2$, the extropolation of M−X bond strengths from one system to another, even with the same metal oxidation state, may not be plausible.[14] With differences in metal oxidation state, agreement is anticipated to be worse. Indeed, all of the aforementioned $Pt^{IV}-CH_3$ bonds strengths are considerably lower than reported $Pt^{II}-CH_3$ bond strengths (242−269 kJ).[15]

For the carbon−iodide coupling reductive elimination reaction, the relationship between the enthalpy and the bond dissociation energies can be expressed as $\Delta H_{C-I} = D(\text{Pt}-CH_3) + D(\text{Pt}-\text{I}) - D(\text{I}-CH_3)$. With our value of $\Delta H_{C-I} = 94$ kJ/mol, the methyl iodide bond dissociation energy of $D(I-CH_3) = 234$ kJ/mol,[10] and the $Pt^{IV}-CH_3$ bond dissociation energy (approximated above) of $D(\text{Pt}-CH_3) = 132$ kJ/mol, the platinum(IV)−iodide bond dissociation energy was found to be $D(Pt^{IV}-I) = 196$ kJ/mol. It is somewhat surprising that the Pt−I bond is estimated to be so much stronger than the Pt−C bond. This difference of $D(\text{Pt}-CH_3) - D(\text{Pt}-\text{I}) = -64$ kJ/mol is much greater than the near zero $D(\text{M}-CH_3) - D(\text{M}-\text{I})$ values found in other systems. Yoneda and Blake reported that $D(\text{Ir}-CH_3) - D(\text{Ir}-\text{I}) = (2 \pm 13)$ kJ/mol for Ir(Cl)(CO)(PMe_3)$_2$(Me)I[6] and Puddephatt and his co-workers found that $D(\text{Pt}-CH_3) - D(\text{Pt}-\text{I}) = (6 \pm 5)$ kJ/mol in *cis*-Pt(PPh_3)$_2$(Me)I.[16]

The above estimations of bond strengths should be qualified by considering the variety of assumptions that were made. These include the approximation of ΔH_{C-I} in the solid state from the solution value (*vide supra*), that no corrections were made for bond energy differences between the starting material and the products, the approximation that the Pt−CH_3 bond strength in the C−I coupling reductive elimination reaction (CH_3 group trans to iodide) is equal to the Pt−CH_3 bond strength in the C−C coupling reductive elimination reaction (average of CH_3 group trans to phosphine and that trans to iodide), and that there is no correction to the gas phase of the DSC results. Some of the general assumptions required in using DSC measurements to obtain bond strength estimates in similar systems have been discussed by others.[5,17]

Kinetics and Activation Parameters of the Methyl Iodide Elimination Reaction. Treatment of the concentration data of **1** and **2** upon approach to equilibrium in the presence of high iodide concentrations allows calculation of the rate constant for reductive elimination of methyl iodide, k_{re}. Integration of the standard kinetic equation of a reversible reaction A ⇌ B + C (eq 2) yields eq 3 ($A_o = [\mathbf{1}]_0$; $X = [\mathbf{2}] = [\text{MeI}]$; $X_e = [\mathbf{2}]_{eq} = [\text{MeI}]_{eq}$; t = time).[18]

$$\frac{dX}{dt} = k_{re}(A_o - X) - k_{ox}X^2 \qquad (2)$$

$$\frac{X_e}{2A_o - X_e} \ln\left[\frac{A_oX_e + X(A_o - X_e)}{A_o(X_e - X)}\right] = k_{re}t \qquad (3)$$

Thus k_{re} can be calculated from the slope of the line generated by plotting $Y = \ln\{[A_oX_e + X(A_o - X_e)]/[A_o(X_e - X)]\}$ versus time (t), and a typical plot is shown in Figure 5. The rate constants (69−99 °C) determined by this method are listed in Table 1. Note that there is no apparent dependence of the rate constant k_{re} on the iodide concentration (Figure 6). The temperature dependence of the rate constants measured fits the Eyring relation, and the apparent activation parameters, ($\Delta H_{re}^{\ddagger} = 104 \pm 1$ kJ/mol and $\Delta S_{re}^{\ddagger} = -12 \pm 1$ J/(mol·K)) were calculated from a plot of $\ln(k_{re}/T)$ versus $(1/T)$ (Figure 7). When these apparent activation parameters for the reductive elimination and the thermodynamic parameters for the reaction are considered together, the activation parameters for the oxidative addition of MeI to **2** are accessible. This is shown in the energy profile of the reaction (Figure 8). Thus the activation parameters $\Delta H_{ox}^{\ddagger}$ and $\Delta S_{ox}^{\ddagger}$ for the oxidative addition of MeI to (dppe)Pt-Me_2 were calculated as $\Delta H_{ox}^{\ddagger} = \Delta H_{re}^{\ddagger} - \Delta H = 38 \pm 4$ kJ/mol and $\Delta S_{ox}^{\ddagger} = \Delta S_{re}^{\ddagger} - \Delta S = -165 \pm 8$ kJ/mol.

Mechanisms of Reductive Eliminations Leading to C−C and C−I Bond Formation. The mechanism most consistent with our results and with previous published work in the field is shown in Scheme 2. Initial reversible loss of iodide from **1**

(8) The validity of both these assumptions is suggested by the reported measurement of $\Delta H_{solution}$(MeI) in 1,2-dichlormethane (1.09 ± 0.04 kJ/mol) and the near identical values of $\Delta H_{solution}$ of the Ir(I) and Ir(III) complexes, IrCl(CO)(PMe_3)$_2$ (17.1 ± 4.1 kJ/mol) and IrCl(CO)(PMe_3)$_2$(Me)(I) (18.6 ± 0.4 kJ/mol) in 1,2-dichloromethane.[6]

(9) Low, J. J.; Goddard, W. A., III *J. Am. Chem. Soc.* **1986**, *108*, 6115.

(10) (a) Benson, S. W. *Thermochemical Kinetics*, 2nd ed.; Wiley: New York, 1976 (b) Benson, S. W. *J. Chem. Ed.* **1965**, *42*, 502.

(11) Roy, S.; Puddephatt, R. J.; Scott, J. D. *J. Chem. Soc., Dalton Trans.* **1989**, 2121

(12) In ref 5 where the Pt-CH_3 bond strength for this compound is reported, the value is given as 144 kJ and this is the numerical value that is extensively referenced in the literature. However, the value was determined using an older CH_3-CH_3 bond strength of 351 kJ/mol. Correction via use of the more recent CH_3-CH_3 bond strength[10] results in a Pt−CH_3 bond strength of 153 kJ/mol.

(13) Egger, K. W. *J. Organomet. Chem.* **1970**, *24*, 501.

(14) Hoff, C. D.; Nolan, S. P.; Stoutland, P. O.; Newman, L. J.; Buchanan. J. M.; Bergman, R. G.; Yang, G. y.; Peters, K. S. *J. Am. Chem. Soc.* **1987**, *109*, 3143.

(15) Martino Simões, J. A.; Beauchamp, J. L. *Chem. Rev.* **1990**, *90*, 629.

(16) Mortimer, C. T.; Wilkinson, M. P.; Puddephatt, R. J. *J. Organomet. Chem.* **1979**, *165*, 265.

(17) (a) Brown, M. P.; Puddephatt, R. J.; Upton, C. E. E.; Lavington, S. W. J. *J. Chem. Soc., Dalton Trans.* **1974**, 1613 (b) Mortimer, C. T.; McNaughton, J. L.; Puddephatt, R. J. *J. Chem. Soc., Dalton Trans.* **1972**, 1265 and references therein.

(18) Laidler, K. J. *Chemical Kinetics*, 3rd ed.; Harper& Row: New York, 1987.

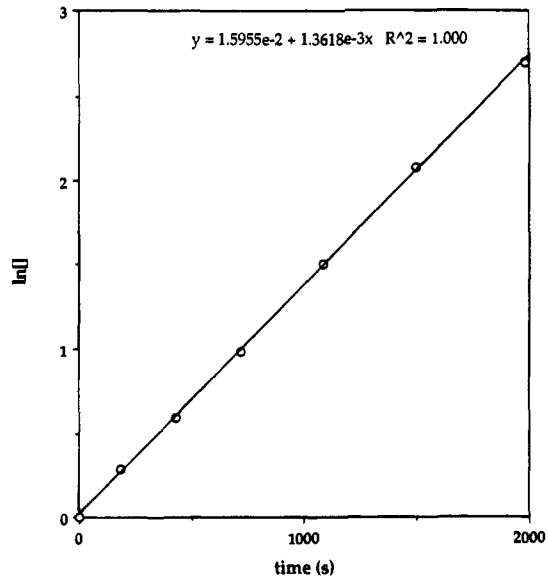

Figure 5. Graph of $\ln\{[A_oX_e + X(A_o - X_e)]/[A_o(X_e - X)]\}$ versus time for the thermolysis of **1** in acetone-d_6 at 79 °C ($[\mathbf{1}]_o = 1.3 \times 10^{-2}$ M, [NaI] = 0.19 M).

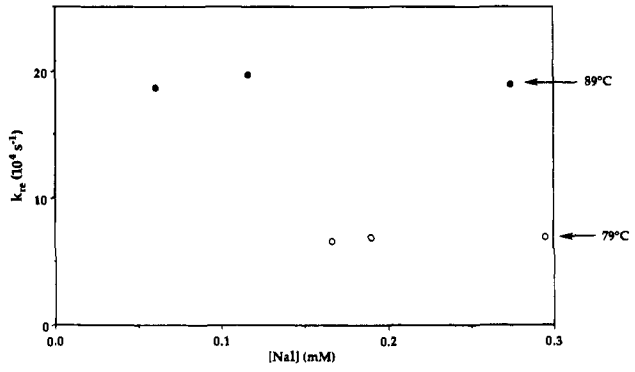

Figure 6. Rate constants k_{re}, for MeI reductive elimination from **1** are shown as a function of [NaI] (79 °C, open circles; 89 °C, filled circles).

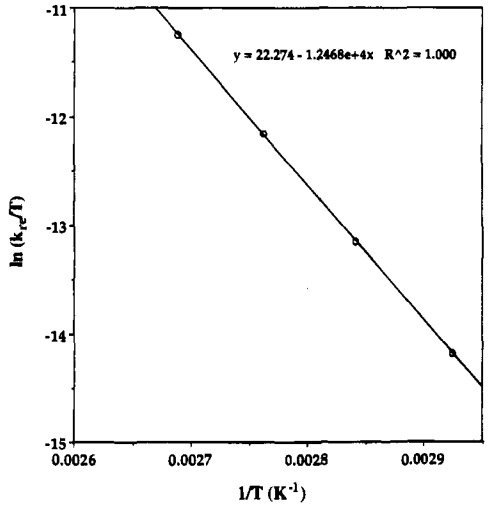

Figure 7. Plot of $\ln(k_{re}/T)$ versus $1/T$ for the reaction **1** → **2** + MeI.

generates the cationic intermediate **A**.[19] Intermediate **A** can then react by three routes: (i) elimination of ethane, (ii) reaction with iodide to form methyl iodide and **2**, or (iii) reaction with iodide to reform **1**. In the presence of excess iodide these latter two pathways are accelerated and dominate, which leads to the

(19) Intermediates **A**, **B**, and **C** may be solvated species (**A′**, **B′**, and **C′**).

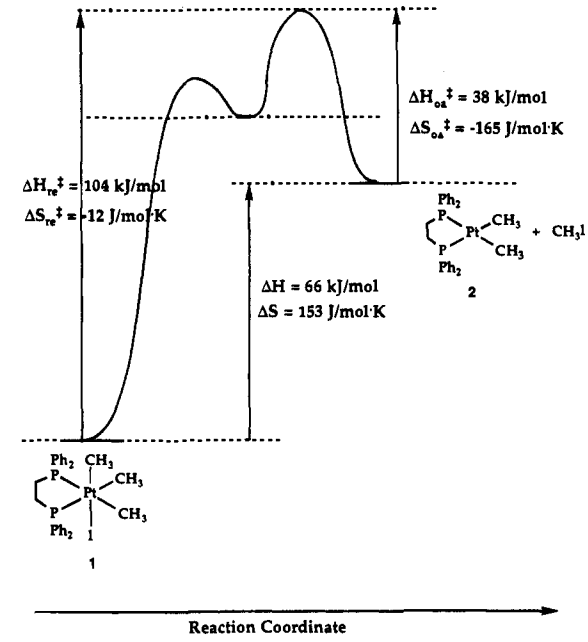

Figure 8. Reaction energy profile for **1** ⇌ **2** + MeI.

Scheme 2

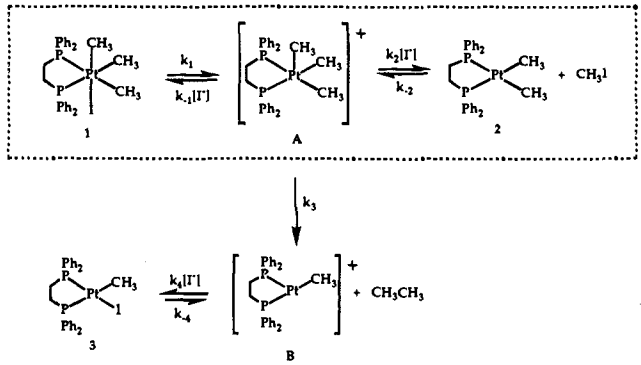

observed equilibrium between **1** and **2**/MeI. However, since the carbon−carbon coupling is the thermodynamically favored pathway, eventually all materials are converted to ethane and dppePtMeI.

The mechanistic pathway proposed for the elimination of methyl iodide is the microscopic reverse of the popular S_N2 mechanism often proposed for oxidative addition of methyl iodide to square planar d^8 metal centers.[20−23] Since under conditions of high iodide concentrations at early reaction times **2** and MeI are the only observed products, k_3 can be neglected which leaves only the boxed part of the scheme for kinetic analysis. Using a steady-state approximation with respect to the cationic intermediate **A** shown in the scheme, the rate equation for the reductive elimination of methyl iodide should show no iodide dependence (eq 4).

$$\frac{-d[\mathbf{1}]}{dt} = k_1[\mathbf{1}] - k_{-1}[\mathbf{A}][I^-] = \frac{k_1k_2[\mathbf{1}] - k_{-1}k_{-2}[\mathbf{2}][CH_3I]}{k_{-1} + k_2} \quad (4)$$

This is consistent with our result that the time required to reach equilibrium was independent of the iodide concentration.

(20) Chock, P. B.; Halpern, J. *J. Am. Chem. Soc.* **1966**, *88*, 3511.
(21) Ugo, R.; Pasini, A.; Fusi, A.; Cenini, S. *J. Am. Chem. Soc.* **1972**, *94*, 7364.
(22) Byers, P. K.; Canty, A. J.; Crespo, M.; Puddephatt, R. J.; Scott, J. D. *Organometallics* **1988**, *7*, 1363 and references cited therein.

Scheme 3

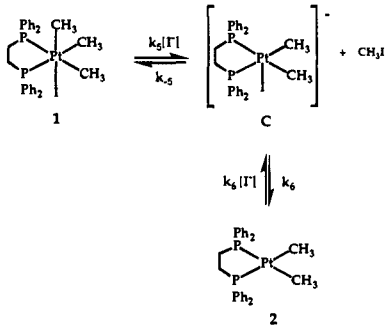

Table 2. Activation Parameters for Oxidative Addition of Methyl Iodide to Square-Planar d^8 Metal Complexes

complex	solvent	$\Delta H^{\ddagger}_{ox}$ (kJ/mol)	$\Delta S^{\ddagger}_{ox}$ (J/(mol·K))	ref
$(PPh_3)_2Ir(Cl)(CO)$	benzene	29	−197	21
	benzene	23	−213	20
	DMF	69	−42	20
$(PEtPh_2)_2Ir(Cl)(CO)$	benzene	41	−142	21
$(PEt_2Ph)_2Ir(Cl)(CO)$	benzene	41	−142	21
$bpyPdMe_2$	acetone	23	−157	22
$bpyPtMe_2$	acetone	22	−138	22
$dppePtMe_2$	acetone	38	−165	this work

Furthermore the rate constants for MeI reductive elimination, k_{re}, showed no dependence on iodide concentration. The lack of augmentation of the rate of methyl iodide elimination in the presence of iodide argues against a mechanism involving direct attack of iodide on **1** to generate methyl iodide and an anionic five-coordinate intermediate as shown in Scheme 3. Such a mechanism would be the microscopic reverse of that which has been postulated for iodide acceleration in the oxidative addition of methyl iodide to rhodium and iridium centers.[24] Kinetic treatment of the iodide accelerated mechanism shown in Scheme 3 using a steady-state approximation with respect to the anionic intermediate **C** produces a rate expression dependent on the iodide concentration (eq 5), and such dependence was not observed.

$$\frac{-d[\mathbf{1}]}{dt} = k_5[\mathbf{1}][I^-] - k_{-5}[\mathbf{C}][CH_3I] = \frac{[I^-](k_5k_6[\mathbf{1}] - k_{-5}k_{-6}[\mathbf{2}][CH_3I])}{k_{-5}[CH_3I] + k_6} \quad (5)$$

Additional support for our proposed mechanism for MeI elimination can be found by comparison of the activation parameters that we calculated for the reverse reaction, oxidative addition of MeI to $dppePtMe_2$, to the published values for the oxidative addition of MeI to other square-planar d^8 systems (Table 2). Evidence collected for these reactions is consistent with a mechanism involving S_N2 nucleophilic attack of the metal center on the MeI and displacement of iodide.[20-23] Subsequent coordination of the iodide to the cationic five-coordinate intermediate occurs in a second step. Although not observed in the Ir systems, the solvated five-coordinate intermediate has been detected by low-temperature NMR in the oxidative addition of MeI to $bpyPtMe_2$ (bpy = bipyridine) in CD_3CN and to $bpyPdMe_2$ in CD_3CN and acetone-d_6[22,25] The close agreement of our activation parameter values for the oxidative addition of MeI to **2**, in particular that of $\Delta S^{\ddagger}$, is suggestive of a similar mechanistic pathway. The reductive elimination pathway as set forth in Scheme 2 is maintained by the principle of microscopic reversibility.

The pathway leading to carbon−carbon coupling reductive elimination as shown in Scheme 2 also has significant literature precedent. In a large number of systems it has been observed that predissociation of an ancillary ligand and concerted elimination from the resulting five-coordinate intermediate occurs preferentially to direct elimination from six-coordinate octahedral d^6 metal complexes.[1,5,22,26] For example, the results of classic mechanistic studies on reductive elimination of ethane from Pt(IV) trimethyl iodide complexes with monodentate phosphines were consistent with a pathway involving preliminary dissociation of phosphine and concerted C−C coupling occurring from a five-coordinate intermediate.[5] Significant rate inhibition was seen when phosphine was added to the reaction. For analogous trimethyl iodide complexes containing neutral bidentate ligands, (e.g., $bpyPdMe_3I$), five-coordinate intermediates have also been invoked in the mechanism of ethane elimination.[22] However, as the chelating nature of the neutral ligand disfavors appreciable dissociation, a five-coordinate cationic intermediate has been proposed to result from dissociation of the iodide. Consistent with this proposal, the rate of elimination was retarded by the addition of iodide. In more recent work, volumes of activation for the reductive elimination of $bpyPdMe_3I$ were measured both in the presence and in the absence of NaI.[27] The similarity of the values led the authors to suggest that ethane elimination occurs not from the five-coordinate intermediate but either from the six-coordinate starting complex or from the more labile six-coordinate solvated cation, $[bpyPdMe_3(S)]^+$ (S = solvent). The presence of NaI suppresses the formation of this latter more labile species and so acts to slow the reaction rate. In the present system it is also clear that carbon−carbon reductive elimination is inhibited in the presence of iodide. As shown in Figure 2, ethane and **3** were present at early reaction times (several minutes at 79 °C) when no iodide was added to the solution. However, in the presence of added iodide, ethane and **3** were not observed until after the methyl iodide equilibrium had been maintained for several hours (Figure 3). In addition, the time that equilibrium was maintained (the time that ethane elimination was suppressed) increased with higher iodide concentrations.

Further support of the cationic intermediate, $dppePtMe_3^+$ (**A**), occurring on the pathway to carbon−carbon reductive elimination from **1** is found by the addition of silver ions to the system. When **1** was treated with $AgBF_4$ (in acetone-d_6), ethane was observed to form immediately upon warming to room temperature. ^1H and ^{31}P NMR signals due to a Pt containing product, consistent with the formulation dppePtMe(S) (S = solvent, shown as **B′** in Scheme 4), were also observed. When NaI was added to the resulting solution, signals due to **B′** were replaced

(23) (a) Kubota, M.; Kiefer, G. W.; Ishikawa, R. M.; Bencala, K. E. *Inorg. Chim. Acta* **1973**, *7*, 195. (b) Thompson, W. H.; Sears, C. T., Jr. *Inorg. Chem.* **1977**, *16*, 764. (c) Burgess, J.; Hacker, M. J.; Kemmitt, R. D. W. *J. Organomet. Chem.* **1974**, *72*, 121. (d) Puddephatt, R. J.; Scott, J. D. *Organometallics* **1985**, *4*, 1221. (e) Crespo, M.; Puddephatt, R. J. *Organometallics* **1987**, *6*, 2548.

(24) (a) Murphy, M. A.; Smith, B. L.; Torrence, G. P.; Aguito, A. *Inorg. Chim. Acta* **1985**, *101*, L47. (b) Hickey, C. E.; Maitlis, P. M. *J. Chem. Soc., Chem. Commun.* **1984**, 1609. (c) deWaal, D. J. A.; Gerber, T. I. A.; Louw, W. J. *Inorg. Chem.* **1982**, *21*, 1259. (d) Forster, D. *J. Am. Chem. Soc.* **1975**, 97, 951.

(25) Byers, P. K.; Canty, A. J.; Skelton, B. W.; Traill, P. R.; Watson, A. A.; White, A.H. *Organometallics* **1992**, *11*, 3085.

(26) (a) Milstein, D. *Acc. Chem. Res.* **1984**, *17*, 221 and references therein. (b) Milstein, D. *J. Am. Chem. Soc.* **1982**, *104*, 5227. (c) Saunders, D. A.; Mawby, R. J. *J. Chem. Soc., Dalton Trans.* **1984**, 2133 (d) Ettore, R. *Inorg. Nucl. Chem. Lett.* **1969**, *5*, 45. (e) de Graaf, W.; Boersma, J.; Smeets, W. J. J.; Speck, A. L.; van Koten, G. *Organometallics* **1989**, *8*, 2907. (f) Basato, M.; Morandini, F.; Longato, B.; Bresadola, S. *Inorg. Chem.* **1984**, *23*, 649. (g) Basato, M.; Morandini, F.; Longato, B.; Morandini, F.; Bresadola, S. *Inorg. Chem.* **1984**, *23*, 3972.

(27) Dücker-Benfer, C.; van Eldik, R.; Canty, A. J. *Organometallics* **1994**, *13*, 2412.

Scheme 4

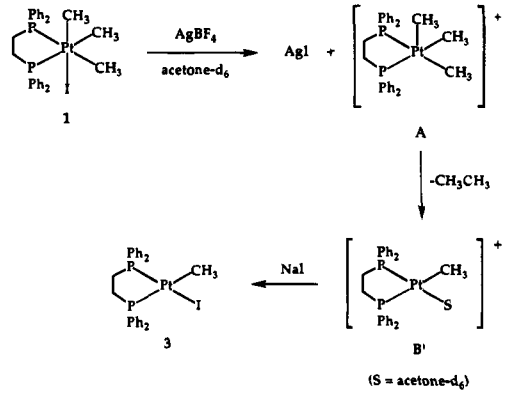

by those of the Pt(II) complex **3**. Thus, as depicted in Scheme 4, removal of iodide from the system (precipitation of AgI) allows formation of the five-coordinate intermediate **A**, which promotes reductive elimination below room temperature. Attempts to observe intermediate **A** (or its solvated form **A'**) by low-temperature NMR have been complicated by low solubility of **1** and the reactivity of **A**. Experiments in other solvents are underway in hopes of increased solubility of the starting complex **1** and greater stability of the intermediate **A'**.

Conclusions

The discovery that the complex dppePtMe$_3$I undergoes a competitive reaction resulting in reductive elimination of both ethane and methyl iodide with concurrent formation of the expected Pt(II) products provided us with a unique opportunity to investigate and directly compare the energetics and mechanisms of C−C and C−I bond forming reductive elimination reactions. It was found that C−C bond formation is greatly favored by thermodynamics ($\Delta H_{C-C} = -105$ kJ/mol versus $\Delta H_{C-I} = 66$ kJ/mol), yet C−I bond formation is kinetically favored. The apparent activation parameters for the reductive elimination of methyl iodide as well as the activation parameters for the oxidative addition of methyl iodide were determined. The energetic parameters are summarized in the energy profile for the reaction (Figure 9). As shown in this energy profile and in Scheme 2, both reactions proceed through a common cationic five-coordinate intermediate formed by dissociation of iodide. It is possible then to tune the competing eliminations to give exclusively C−I or C−C coupling by the addition or removal of iodide (using Ag^+) from the system.

The mechanism proposed for the reductive elimination of methyl iodide is the microscopic reverse of the popular S_N2 mechanism accepted for the oxidative addition of methyl iodide to square-planar d^8 metal complexes. The activation parameters and the lack of an effect of added iodide on the rate of reaction support this mechanism for methyl iodide elimination.

The mechanism proposed for the reductive elimination of ethane is similar to those proposed previously for reductive elimination of ethane from six-coordinate d^6 metal complexes of Pt and Pd. Reductive elimination occurs from a five-coordinate intermediate formed by preliminary dissociation of a ligand rather than directly from the six-coordinate starting complex.[5,11,22] It is perhaps significant to generalize the results of these studies with ours as shown in Scheme 5. If neutral monodentate ligands are present, dissociation of a neutral ligand is a low-energy pathway to a five-coordinate intermediate. If the neutral ligand is chelating, a higher energy process resulting in charge separation must occur and an anion dissociates to form the five-coordinate intermediate. Rationalizations for the role of an open coordination site and the importance of a five-

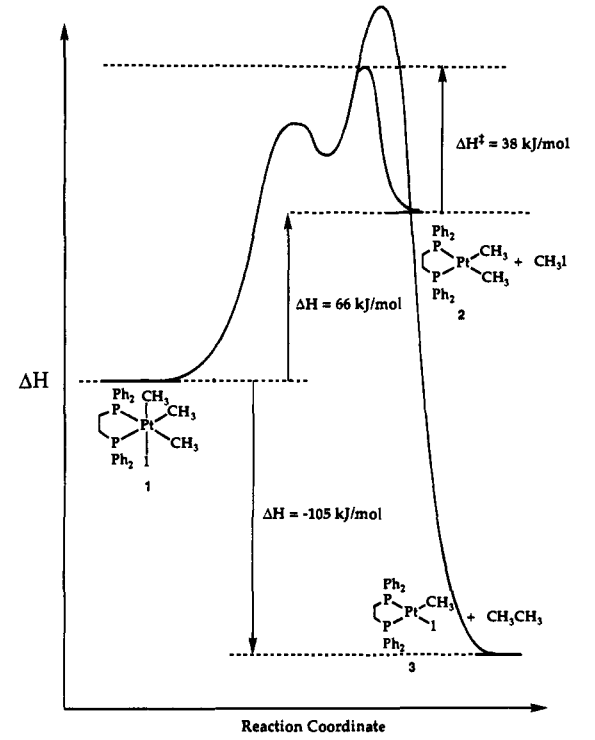

Figure 9. Reaction energy profile for the conversion of **1** to **2**/MeI and **3**/CH_3CH_3.

Scheme 5

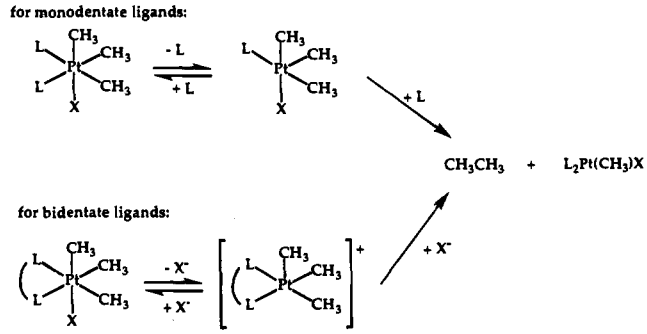

coordinate intermediate in this process, including the possibility of involvement of an agostic C−H interaction, have been discussed elsewhere.[5,11,22] An alternative explanation that reductive elimination occurs from the six-coordinate solvated form of the intermediate has also been offered.[27]

Experimental Section

General Procedures. Reactions under N_2 were carried out in a Vacuum Atmospheres VAC-MO-20 drybox. ^{1}H NMR and ^{31}P NMR spectra were obtained on a Varian Gemini System 300 MHz Fourier transform spectrometer. ^{1}H NMR spectra were recorded relative to residual protiated solvent and chemical shifts are reported in units of parts per million downfield from tetramethylsilane. ^{31}P NMR spectra were obtained at 121.4 MHz and referenced to an external standard of 85% H_3PO_4; ^{31}P NMR are reported in parts per million downfield from H_3PO_4. All coupling constants are reported in hertz.

Unless otherwise noted, all samples were weighed on a Mettler Instrument AG-UM3 analytical balance. Elemental analyses were carried out by Micro-Analysis Inc., Wilmington, DE. Solid state DSC experiments were monitored using a Perkin-Elmer DSC7 differential scanning calorimeter with TAC 7/DX thermal analysis controller. Perkin-Elmer aluminum sample pans (No. 219-0041) were used in these experiments and were left uncrimped. Solid state TGA experiments were monitored using a Perkin-Elmer TGA7 thermogravimetric analyzer with TAC 7/DX thermal analysis controller, using a platinum sample

pan. The data were collected and analyzed by an IBM Personal System Model 50Z computer with Perkin-Elmer DSC/TGA software.

Kinetic and thermodynamic experiments were run in flame-sealed NMR tubes, and the samples were heated in a Neslab EX-250 HT high-temperature oil bath. Sealed NMR tubes were prepared by attaching Wilmad 504-PP medium-walled NMR tubes to Kontes vacuum stopcocks via cajon adapters.[28] The volume of solution in the 504-PP NMR tubes was measured by comparison to a previously calibrated tube.

Unless otherwise specified, all reagents were purchased from commercial suppliers and used without further purification. Methyl iodide was stored under activated 4 Å molecular sieves with Cu and protected from light. Acetone-d_6 was degassed and dried with activated 4 Å molecular sieves. Ferrocene (Aldrich) was sublimed prior to use.

Preparation of dppePtMe$_3$I (1). This compound was prepared either by oxidative addition of CH_3I to dppePtMe$_2$ (**2**)[29] or by reaction of $[PtMe_3I]_4$ with dppe.[5] Recrystallization of the product from CH_2Cl_2/pentane resulted in white crystalline product containing 1 equiv of CH_2Cl_2. Solvent-free material was obtained by dissolving **1**·CH_2Cl_2 in benzene and precipitating the product as a white solid with pentane. ^{1}H NMR: ($CDCl_3$) δ 0.48 (t with Pt satellites, 3H, J_{Pt-H} = 69.2, J_{P-H} = 7.5), 1.60 (t with Pt satellites, 6H, J_{Pt-H} = 59.7, J_{P-H} = 6.8), 3.0 (m, 4H) 7.35 (multiplet, 4H), 7.73 (multiplet, 16H); (acetone-d_6) δ 0.36 (t with Pt satellites, 3H, J_{Pt-H} = 69.2, J_{P-H} = 7.3), 1.52 (t with Pt satellites, 6H, J_{Pt-H} = 59.8, J_{P-H} = 6.7), 3.2 (m, 4H), 7.40 (m, 12H), 7.52 (m, 4H), 7.84 (m, 4H). ^{31}P NMR (acetone-d_6) δ 7.41 (s with Pt satellites, J_{P-Pt} = 1112). Elemental Anal. for $C_{29}H_{33}IP_2Pt$: C, 45.50; H, 4.34. Found: C, 45.53; H, 4.43. Literature values: ^{1}H NMR ($CDCl_3$) δ 0.49 (t, 3H, J_{Pt-H} = 69.4, J_{P-H} = 7.5), 1.62 (6H, J_{Pt-H} = 60.0), 2.97 (m, 4H). Elemental Anal. for $C_{29}H_{33}IP_2Pt$: C, 45.9; H, 4.4.[29]

Differential Scanning Calorimetry Studies. In a typical DSC experiment, an empty aluminum pan and lid were weighed on an analytical balance. (dppe)PtMe$_3$I (*ca.* 3 mg) was then added to the pan and pan and lid were re-weighed to determine the amount of sample to microgram accuracy. The sample was heated in the DSC at 5 °C/min from 50 to 200 °C. The composition of the solid residue that remained after heating was examined by ^{1}H NMR ($CDCl_3$). The Pt-CH_3 signals for **2** (δ 0.70, t with Pt satellites, 6H, J_{Pt-H} = 70.5, J_{P-H} = 7.3) and for **3** (δ 0.89, dd with Pt satellites, 6H, J_{Pt-H} = 59.0, J_{P-H} = 4.7, 7.3) were integrated relative to one another.

Thermogravimetric Analysis Studies. In a typical TGA experiment, (dppe)PtMe$_3$I (*ca.* 3 mg) was placed in the platinum TGA sample pan. The weight of the starting material was directly read from the balance of the TGA instrument. The TGA was heated at 5 °C/min from 50 to 200°C . After the TGA experiment was completed, the composition of solid residue was examined by ^{1}H NMR ($CDCl_3$) as described above for DSC experiments.

Reductive Elimination Reactions in Acetone-d_6. In a typical experiment, (dppe)PtMe$_3$I (4.763 mg, 6.22 × 10^{-3} mmol), Cp_2Fe (0.554 mg, 2.98 × 10^{-3} mmol, internal standard), and NaI (22.135 mg, 0.1477 mmol) were weighed on an analytical balance, mixed in a small vial, and dissolved in acetone-d_6. The solution was transferred to an NMR tube and the solvent was carefully removed under vacuum. Acetone-d_6 (from 4 Å sieves) was transferred into the NMR tube under vacuum and the tube was flame sealed. The sample was warmed to room temperature and the volume of the solution was measured (V = 0.50 mL). After an initial ^{1}H NMR spectrum was recorded, the tube was heated at a specified temperature in an oil bath. At given intervals, the tube was taken out of the bath, cooled quickly to −78 °C and kept in liquid nitrogen until a ^{1}H NMR spectrum could be recorded. The sample was thawed and the ^{1}H NMR spectrum was recorded at 21 °C. The NMR tube was then returned to the oil bath for additional heating. To analyze the reaction progress: The starting material and products signals were integrated against the internal standard (Cp_2Fe) signal (δ = 4.11, singlet, 10H). The concentration of Cp_2Fe was adjusted by the dppePtMe$_3$I initial concentration (due to Cp_2Fe sublimation under vacuum before the NMR tube was sealed). The ratio of the integration of the central triplet at δ 1.52 (two CH_3 groups trans to phosphine in dppePtMe$_3$I which did not contain ^{195}Pt, 6H, 66.2% of total dppePtMe$_3$I) to the integration of Cp_2Fe signal provided the molar ratio of these two species. The concentration of starting material was then calculated by multiplying this molar ratio by the Cp_2Fe concentration. The concentration of dppePtMe$_2$ was similarly calculated by integration of the central triplet at δ 0.59 (CH_3 groups not attached to ^{195}Pt, 6H, 66.2% of total dppePtMe$_2$). The central doublet of doublets of the (dppe)-PtMeI product (δ 0.80) overlapped with the C_2H_6 signal, so that the concentration of (dppe)PtMeI was calculated either by deducting the dppePtMe$_3$I and dppePtMe$_2$ concentrations from the total concentration of the platinum species or by the integration of its platinum satellite (doublet of doublets at δ 0.90 (3H, 50% of ^{195}Pt product, 16.9% of total dppePtMeI) against Cp_2Fe as described above. This latter direct method could be used more effectively as the concentration and intensity of the signal increased. The data were collected at least until the carbon−carbon coupling products dppePtMeI/MeMe began to appear, or until all the platinum species were converted to the dppePtMeI/MeMe final products.

Reaction of 1 with AgBF$_4$. Under N_2, **1** (4.6mg, 6.0 × 10^{-3} mmol) and $AgBF_4$ (2.5 mg, 1.3 × 10^{-2} mmol) were placed in an NMR tube. Acetone-d_6 (0.38 mL) was vacuum transferred into the tube and the tube was sealed immediately. ^{1}H NMR [δ 0.82 (s, ethane), δ 0.36 (d (broad) with Pt satellites, J_{P-H} = 7.1, J_{Pt-H} = 47.6)] and ^{31}P NMR [δ 60.1 (s, with Pt satellites, J_{Pt-P} = 1817); 40.0 (s, with Pt satellites, J_{Pt-P} = 4616)] were recorded. The tube was opened under vacuum and the volatile materials were transfered to another NMR tube which was then sealed under vacuum. A ^{1}H NMR spectrum of the volatiles tube clearly showed ethane [δ 0.82]. To the solid residue from the original tube was added acetone-d_6, and this solution was filtered through glass wool. To the filtrate was added NaI (5.0 mg, 3.3 × 10^{-2} mmol). ^{1}H NMR and ^{31}P NMR both indicated the presence of dppePtMeI (**3**) [^{1} H NMR: δ 0.80 (dd with Pt satellites, J_{P-H} = 4.5, 7.3, J_{Pt-H}= 59.5); ^{31}P NMR: δ 51.7 (s, with Pt satellites, J_{Pt-P} = 4023), δ 50.6 (s, with Pt satellites, J_{Pt-P} = 1748)].

Acknowledgment is made to the donors of the Petroleum Research Fund, administered by the American Chemical Society, for partial support of this research. We are also grateful for a generous loan of K_2PtCl_4 from Johnson Matthey/Aesar/Alfa and to the referees of this manuscript for their insightful comments. R. K. Bunting and C. D. Stevenson are acknowledged for helpful discussion.

JA942692V

(28) Bergman, R. G.; Buchanan, J. M.; McGhee, W. D.; Periana, R. A.; Seilder, P. F.; Trost, M. K.; Wenzel, T. T. In *Experimental Organometallic Chemistry: A Practicum in Synthesis and Characterization*; Wayda, A. L., Darensbourg, M. Y., Eds.; ACS Symposium Series 357; American Chemical Society: Washington, DC, **1987**; p 227.

(29) Appleton, T. G.; Bennett, M. A.; Tomkins, B. *J. Chem. Soc., Dalton Trans.* **1976**, 439.